

Investigation of the properties of single-step and double-step grown ZnO nanowires using chemical bath deposition technique

Somdatta Paul¹, Avishek Das², Mainak Palit¹, Satyaban Bhunia³, Anupam Karmakar², Sanatan Chattopadhyay^{1,2,*}

¹Centre for Research in Nanoscience and Nanotechnology (CRNN), University of Calcutta, Kolkata 700098, India

²Department of Electronic Science, University of Calcutta, Kolkata 700009, India

³Saha Institute of Nuclear Physics, Kolkata 700064, India

*Corresponding author. Tel: (+91) 9432082727; E-mail: scelc@caluniv.ac.in

Received: 14 November 2015, Revised: 21 December 2015 and Accepted: 22 May 2016

ABSTRACT

In this work, a comparative performance analysis of ZnO nanowires grown by following single- and double-step techniques on (100) p-Si substrate has been conducted. High-quality ZnO nanowires with c-axis orientation and perfect crystalline structures with appropriate chemical stoichiometry have been obtained from both the approaches. The areal density of the nanowires grown from double step approach is almost twice the nanowires grown by employing the single step approach. Histogram analysis shows that the diameter and height of majority of the single-step grown nanowires are ~ 370 nm and ~ 2.45 μ m, and for the double step grown nanowires these are ~ 210 nm and ~ 2.16 μ m, respectively. The bandgap values of the single-step and double-step grown nanowires are measured to 3.19 eV and 3.26 eV, respectively. The current-voltage characteristics of p-Si/n-ZnO diodes indicate that the forward current is contributed by both the electrons and holes and the relevant cut-in voltages are measured to be 0.5 V and 2.5 V, respectively. Copyright © 2016 VBRI Press.

Keywords: ZnO nanowire; CBD; seed layer; single-step growth; double-step growth.

Introduction

ZnO nanostructures are gaining more and more attention from researchers around the globe due to its wide spread applications in the areas of optoelectronics, piezo-electric, sensing and antibacterial medicines [1-8] and therefore it has renewed the interests for developing further insight to the physical, electronic and optoelectronic properties of ZnO [9]. There are reports on different variant of ZnO nanostructures including nanowires, nanotubes, nanobelts, nanopropellers, and nanocages [10-14]. Among these, the vertical ZnO nanowires are of particular interest due to their unique defined geometry and prospects for developing electron field emitters, vertical transistors, UV LEDs and lasers [15-20]. Several chemical, electrochemical and physical deposition techniques have been explored which include the chemical vapor deposition (CVD) [21], vapor-liquid-solid (VLS) [22], pulsed laser deposition (PLD) [23], spray pyrolysis [24], sputtering [25], electro-deposition [26], molecular beam epitaxy (MBE) [27], sol-gel [28] method and chemical bath deposition (CBD) [29] techniques for the growth of device quality ZnO nanostructures. Out of these, the chemical bath deposition technique is most widely used due to its simple, low temperature, low cost, catalyst free and eco-friendly growth mechanism.

Majority of the reported works are focused on the growth of ZnO nanowires on Si substrate by double-step CBD

approach. However, no successful report is available on the growth of vertical ZnO nanowires on Si substrate by following a single-step CBD route. Some reports are available which demonstrate the growth of highly textured cones or flower-like and columnar crystalline ZnO structures on glass substrates in aqueous ammonia solution by following a single-step CBD approach [30, 31]. The successful growth of ZnO nanostructures on Al₂O₃ substrates [32] and n-GaN substrates has also been reported [33]. However, the synthesis of device quality ZnO nanostructures over large area, which can be integrated with Si, by employing a relatively simple and low-cost approach would always be beneficial to bring ZnO nanowires to the mainstream electronics.

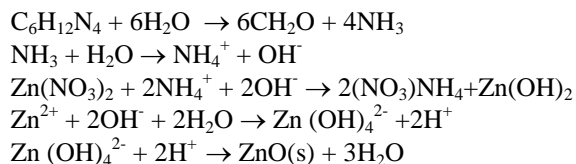
In the current work, the vertically aligned ZnO nanowires on p-Si (100) substrates have been grown by employing both single-step chemical bath deposition (CBD) technique and a double-step deposition approach with sol-gel seed-initiated CBD process for investigating their comparative performance. The relevant growth mechanisms for both the techniques have been addressed. Crystalline nature and orientation of the grown nanowires have been studied with field emission scanning electron microscope (FESEM) and x-ray diffraction (XRD) study. The histogram analyses are done to observe size and height distributions of the nanowires, grown by following the single- and double-step approaches. The photoluminescence spectra of the grown samples have been studied to compare their defect levels

and the average band-gap is estimated from optical absorption spectra. Their chemical composition is determined from energy dispersive x-ray diffraction spectrometry (EDAX) analyses. Finally, electronic transport behavior of the hetero-junctions fabricated using both type of samples is investigated by measuring current-voltage characteristics across it.

Experimental

Synthesis of ZnO nanowires by single- and double-step CBD techniques

The ZnO nanowires are grown on p-Si (100) substrates. Prior to the growth process, the Si wafers (100) are cleaned sequentially with TCE, acetone, iso-propyl alcohol and DI water, followed by a 5-min ultrasonic cleaning. The nanowires are grown by following two different approaches: the single-step and double-step growth. For the single step growth, the blank p-Si wafer is used while for the two-step growth approach, initially a ZnO seed layer is prepared by employing sol-gel route where 5mM Zinc Acetate Di-hydrate ((CH₃COO)₂Zn.2H₂O) is dissolved in 50ml of pure ethanol. The solution is stirred at 450rpm for 5min at room temperature, thereby, forming ZnO nanoparticles [33]. The solution is spin-coated on Si substrate at 500rpm for 30sec, followed by another spin at 2000rpm for 30sec. After the preparation of seeds on Si substrate, these were annealed at 250 °C in Ar environment at 10psi pressure for 30min to remove the solvents. The entire process is repeated for a couple of times to increase the density of nano-particle seeds on Si surface. The nanowires on both the bare as well as seed-coated Si substrates are grown by employing CBD technique. For this purpose, equi-molar aqueous solutions of 0.1M Zinc Nitrate Hexahydrate (Zn(NO₃)₂.6H₂O) and HMTA (C₆H₁₂N₄) are prepared using 50ml of DI water and then mixed together in a beaker which produces a transparent solution. Both the bare and seed-coated Si samples are dipped vertically in the solution using a sample holder and the bath is covered by a heat insulator and stirred at 250rpm. With increasing time and temperature, the transparent solution turns out to be slightly whitish due to the precipitation of ZnO which finally leads to heterogeneous reaction and deposition of ZnO on Si substrate [30]. The deposition was performed for 120min at 90 °C. The solution pH at this stage was measured to be 5.3. The samples are taken out and rinsed immediately in running DI water, followed by drying up in N₂ ambient. The relevant reaction mechanism can be described as follows:



The growth of ZnO nanostructures involves two mechanisms, the nucleation growth and particle growth [30]. During such reaction, HMTA provides OH⁻ ions to the solution by its thermal decomposition, followed by the formation of Zn(OH)₄²⁻ at an intermediate stage which subsequently converts to solid ZnO with the increase of

temperature and time by dehydration reaction. With increasing time, the heterogeneous nucleation of ZnO on Si increases and gradually forms the seeds on Si surface. The non-uniform dangling bonds on silicon surface act as the nucleation sites for ZnO nuclei and such process can be considered as the self-seeding of ZnO. Till date no such self seeding observation has been reported using CBD technique, however, it has been observed by Jeong *et al* using metal-vapor-deposition technique [35]. With continuous supply of ZnO nuclei, additional seeds are formed randomly on the Si surface which also increases size of the seeds. ZnO is a polar crystal having a dipole moment along c-axis [36]. Moreover, growth rate of its [001] plane is the highest [37] and thus having the maximum surface energy. Consequently, the ZnO nanowires grow at a faster rate along <001> direction due to dipole alignment and to minimize the relevant surface energy along c-axis [38]. The nanowires grow epitaxially on such lattice matched ZnO seeds and it should be noted that its growth direction depends on crystallographic orientation of the seeds.

Physical and electrical characterizations of the nano-structures and hetero-junctions

The surface morphology and thickness of the grown samples are characterized by using field emission scanning electron microscopy (FESEM) (Zeiss Auriga 39-63) technique. The analysis of structural and crystallographic orientation of the grown samples is conducted by employing x-ray diffraction (XRD) method. The elemental as well as compositional analysis of the nanowire is performed using energy dispersive x-ray diffraction spectrometry (EDAX, JEOL-JSM 7600F). The bandgap of the grown samples is measured using UV-VIS-NIR absorption spectrophotometer from PerkinElmer, Lambda 1050. The photoluminescence spectra of the grown samples are measured in a SAQ2 spectrometer. The current-voltage characteristics of the p-Si/n-ZnO NW diodes are measured by using Keithley 4200-SCS parameter analyzer.

Results and discussion

Fig. 1(a) and **(b)** shows the SEM micrographs of ZnO nanowire arrays grown by both single-step and double-step approaches on Si (100) substrate, respectively. It is noticed that the grown nanowires in both the techniques acquire a similar hexagonal shape along c-axis plane. In single-step growth, along with the quasi-aligned vertical ZnO hexagonal nanowires, some tipped-nanowires (nano-tips) are also observed with average diameter of ~163nm. In case of double-step growth, the grown nanowires are highly aligned in vertical direction, confirming the c-axis oriented growth. The average diameter of the grown ZnO nanowire is ~210nm and its average height measured from the silicon surface is observed to be ~2.16µm. Also, the areal density of ZnO nanowires grown by the double-step approach is much higher compared to the single-step grown samples, which is attributed to the presence of higher nucleation sites for nanowire growth on the seed layer. The development of reliable electronic devices with uniform characteristics requires precise control of the nanowire sizes since the

electronic transport properties of such structures strongly depend on it.

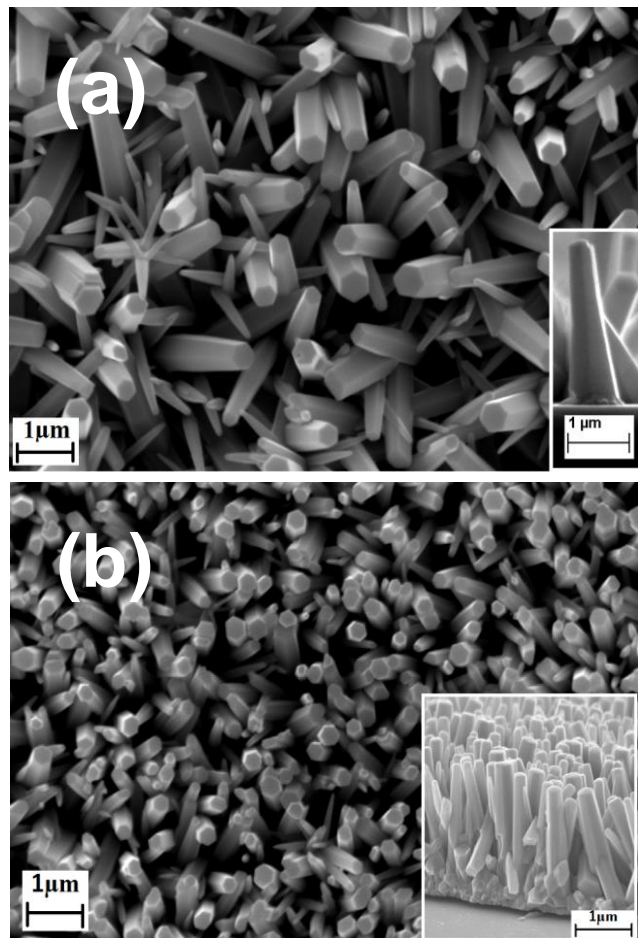


Fig. 1. FESEM images of the ZnO nanowires grown by: (a) single-step approach and, (b) double-step route. Images at the inset show side view of the nanowires.

In this context, the histogram analysis of size distributions of nanowire samples grown by both single-step and double-step approaches is performed and plotted in **Fig. 2 (a)** and **(b)**, for the distribution of diameters, and **(c)** and **(d)**, for the distribution of heights, respectively. It is apparent that the diameter of the ZnO NW's grown by single step ranges from 125nm to 575nm and for the double step it ranges from 75nm to 350nm. The diameter and height of majority the single-step grown nanowires are measured to be ~ 370 nm and ~ 2.45 μm , respectively, as observed from the size distribution of **Fig. 2 (a)** and **(b)**. The similar values for the double-step grown samples are obtained to be ~ 210 nm and ~ 2.16 μm , respectively. Thus, $\sim 8.93\%$ of the grown nanowires following single-step approach will be having diameter in the range of 350-400nm and that for the sample grown by double-step approach is 25.81% in the range of 200-250nm. This is to be noted that all the growth parameters such as molar concentration, solution temperature, and growth time are maintained to be constant to 0.1M, 90 °C and 120min, respectively. The ZnO nanowires are simultaneously grown on both the blank as well as seed-coated Si substrates by dipping in the chemical bath solution. The densely distributed ZnO seeds promote the growth of high density

of nucleation sites for the double-step grown nanowires [39]. Reports are available where the concentration of local Zn^{2+} ions at the vicinity of highly dense growing nanowires (on seed coated substrate) gets reduced due to its higher consumption. In comparison, the localized concentration of Zn^{2+} ions in the vicinity of relatively less densely grown nanowires (single-step grown) is much higher [39, 40]. Consequently, the growth rate of double-step grown nanowires is relatively slower than the single-step grown nanowires, resulting to higher lengths of the nanowire. Moreover, there is less space available in between the densely grown nanowires in double-step approach, which leads to lower diffusion rate of Zn^{2+} ions, thereby, resulting to a relatively slower growth of nanowire side walls [40]. Thus, it makes the double-step grown nanowires comparatively thinner than the single-step grown ZnO nanowires.

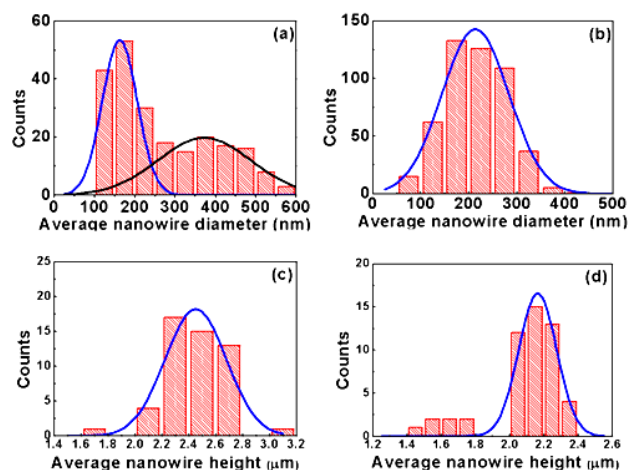


Fig. 2. The plots of dimensional distributions of the ZnO nanowires: (a) distribution of diameters for single-step grown; (b) distribution of diameters for double-step grown; (c) distribution of heights for single-step grown and; (d) distribution of heights for double-step grown. Solid lines show the Gaussian-fit of the distributions.

The chemical compositions of the samples grown by following both single-step as well as double-step routes have been determined by employing EDAX analysis. The presence of Zn and O in EDAX plots of **Fig. 3(a)** confirms the formation of ZnO nanowires. The EDAX pattern also exhibits some elemental trace of Si for the samples grown by single-step approach. Such elemental trace is appearing from Si substrate due to the formation of low density of nanowires on it has been seen from **Fig. 1 (a)**. No such trace of Si is observed for the densely grown ZnO nanowires by double-step route. The atomic fraction of Zn:O in the composition is estimated to be 0.968 and 1.0 for the samples obtained from the double- and single-step routes, respectively, and indicate the growth of nanowires with appropriate stoichiometry.

X-ray diffraction pattern of the ZnO nanowires grown by both single- and double-step approaches are compared in **Fig. 3(b)**, which suggests the formation of wurtzite ZnO nanostructures. The peaks in the graph correspond to polycrystalline ZnO with [002] plane at $2\theta = 34.4^\circ$, which is consistent with the JCPDS card no 36-1451 [41]. The dominant peak in the XRD pattern of single-step grown sample is emerging from [101] plane, indicating

the suppressed c-axis growth. However, the dominant peak for double-step grown samples appears from [002] orientation which indicates c-axis or $\langle 001 \rangle$ growth direction, confirming high crystalline nanowires. These observations are consistent with SEM micrographs where the areal density of double-step grown nanowires is dense and vertically oriented than in case of single-step growth.

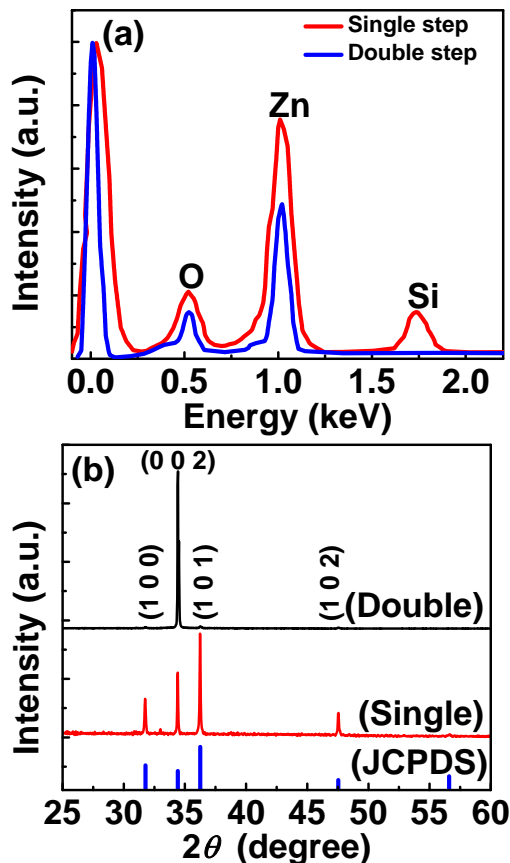


Fig. 3. (a) Energy dispersive x-ray spectroscopy pattern of the ZnO nanowire array grown by single-step and double-step approach (b) Comparative plots of the XRD pattern.

Fig. 4(a) shows the comparative plots of absorption spectra of ZnO nanowires grown by following both single- and double-step approaches. As expected, the spectra reveal that the grown ZnO nanowires have absorption band in UV region, resembling its bandgap. The bandgap is extracted by using Tauc's relation as illustrated at the inset of **Fig. 4(a)** and it is obtained to be 3.19eV for the single-step grown samples and 3.26eV for the double-step grown samples, which are in consistent with the other reported results [42].

However, the single-step grown ZnO nanowires exhibit a relatively lower value of bandgap compared to the double-step grown samples. This is worth pointing that the single-step grown nanowires are directly grown on p-Si substrate and there is 39.1% lattice mismatch between the (100) Si and (001) ZnO nanowires. Such significant lattice mismatch incorporates a significant amount of stress into the nanowires which may cause a reduction of bandgap of these nanowires [43, 44]. The photoluminescence spectra, shown in **Fig. 4(b)**, also revealed that strong UV peak at 380nm corresponds to the near-band edge emission (NBE) due to

recombination of free exciton [45]. The green or deep level emission (DLE) centered at 553nm and 561nm for double- and single-step grown samples are attributed to oxygen vacancies and interstitial zinc [46].

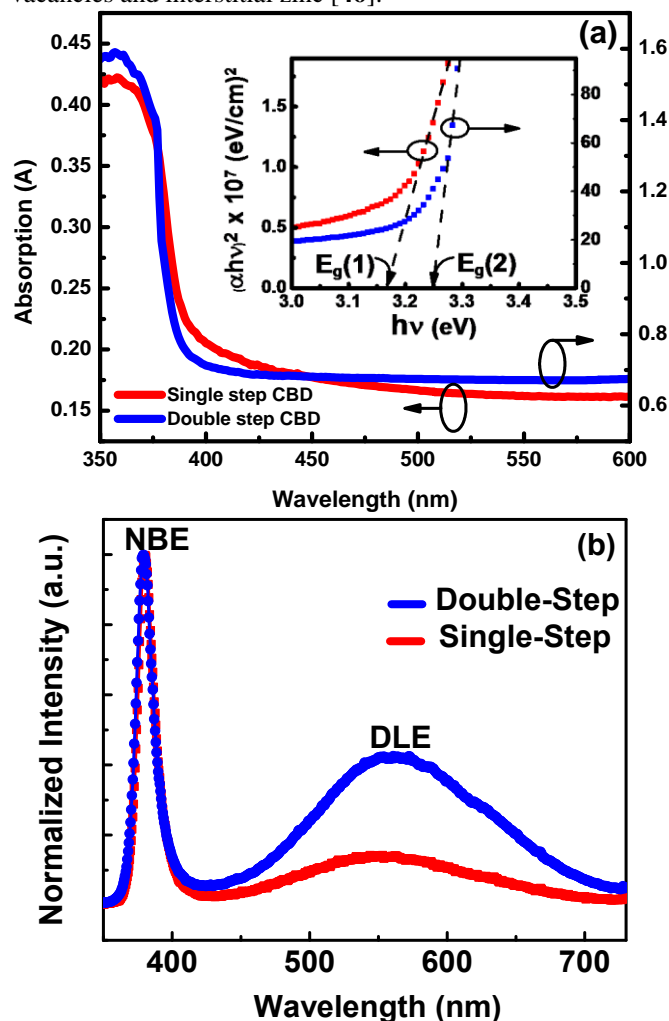


Fig. 4. (a) Comparative plots of absorption with wavelength for the single-step and double-step CBD grown ZnO nanowires. Inset shows the Tauc's plot of the relevant absorption spectra, (b) Room temperature photoluminescence spectra of ZnO nanowires.

The current-voltage characteristics of p-Si/n-ZnO nanowires grown by following both the single and double-step approaches are plotted in **Fig. 5(a)**. The relevant band alignment is also shown at the inset of **Fig. 5(a)**. The calculated average contribution of current per nanowire has been plotted for both the single as well as the double step grown sample in **Fig. 5(b)**. It is observed from the band diagram that a valence band offset (ΔE_V) of 2.6eV and a conduction band offset (ΔE_C) of 0.315eV exist at the hetero-interface of such a nanowire diode and the characteristics exhibit a prominent hetero-junction behavior. It should be noted that the positive bias is applied to p-Si side and the n-ZnO nanowire side is grounded. Therefore, in such a structure, both electron and hole current contribute to the total forward current, where the cut-in voltages for electron and hole transport are different and it is measured to be 0.5V and 2.5V, respectively. This is attributed to the difference in conduction and valence band discontinuities at the hetero-junction of p-Si/n-ZnO

band structure, as observed in Fig. 5(a). The valance band discontinuity is much larger than that of conduction band, thereby, impeding the hole transport below 2.5V and above it, the transport is mainly carried out by holes. The forward current below 2.5V is dominated by the electrons which are injected from gate terminal and the conduction offset at n-ZnO/p-Si hetero-junction favors such electron transport. However, the doping level of p-Si ($4.9 \times 10^{18} \text{ cm}^{-3}$) is higher than n-ZnO ($2.9 \times 10^{16} \text{ cm}^{-3}$) and as a result, the value of hole current becomes almost 2 orders higher than electron current when the applied bias is higher than cut-in voltage.

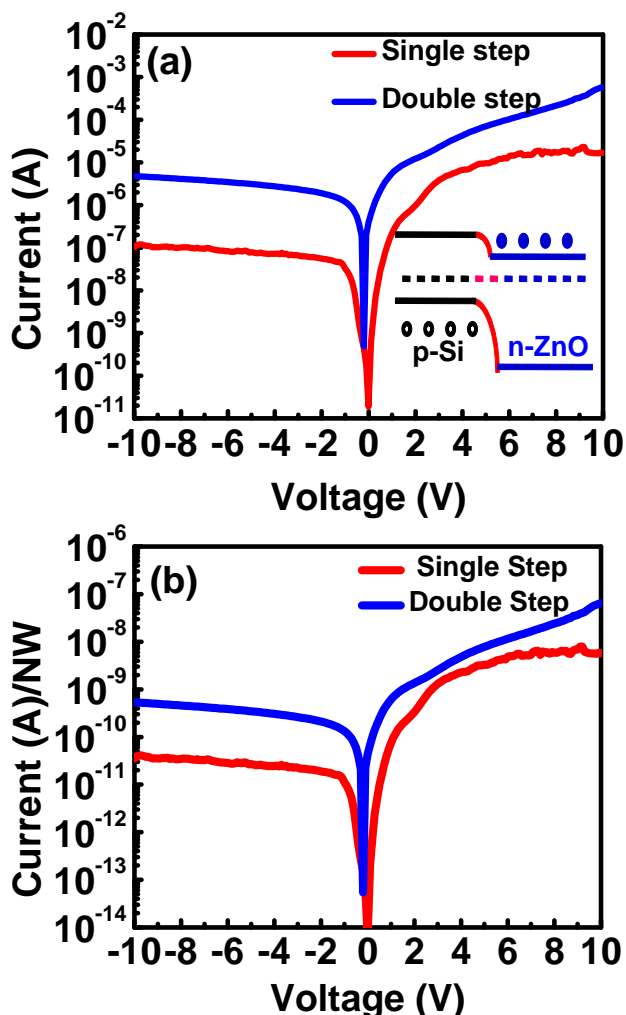


Fig. 5. (a) Comparison of I-V characteristics of n-ZnO NW/p-Si diode. Inset shows the band-diagram of p-Si/n-ZnO (b) Plot shows the current/nanowire of n-ZnO NW/p-Si.

Conclusion

A comparative study has been performed on the growth of ZnO nanowires following single- and double-step approaches, and the high-quality ZnO nanowires with c-axis orientation, appropriate crystalline structure and chemical stoichiometry have been obtained from both the processes. The bandgap of single-step and double-step grown nanowires is estimated to be 3.19eV and 3.26eV, respectively. The nanowires grown by single-step process are initiated by self-seeding of nucleation centers whereas the double-step process is initiated by self-forming

mechanism. The areal density of single step grown nanowires is $2.65 \mu\text{m}^{-2}$ and that of double step is $5.76 \mu\text{m}^{-2}$. This shows the density of the double-step grown nanowires is almost double than those of single-step grown due to already present dense nano-particle seeds, created by sol-gel and spin-coating techniques. Diameter of majority of the single-step grown nanowires is measured to be $\sim 370 \text{ nm}$ and the same for double-step grown nanowires is obtained to be $\sim 210 \text{ nm}$. The current-voltage characteristics indicate that the forward current for both type of samples is contributed by both electrons and holes. The electron and hole cut-in voltages are obtained to be 0.5V and 2.5V, and the conduction and valence band offsets are obtained to be 0.315eV and 2.6eV, respectively.

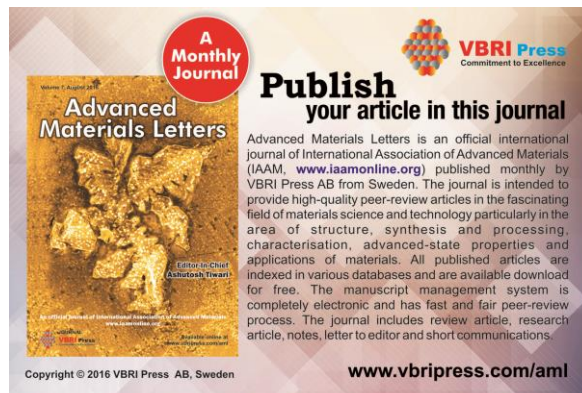
Acknowledgements

Somdatta Paul and Avishek Das like to acknowledge the University Grants Commission (UGC), India, for providing financial support to pursue their research and Mainak Palit acknowledges the Technical Education Quality Improvement Program (TEQIP), World Bank, for the financial support of his research. The authors would also like to acknowledge the DST Purse program and Center of Excellence (COE), TEQIP for providing financial support to setup the electrical characterization laboratory.

Reference

- Hassan, J.J.; Mahdi, M.A.; Yusof, Y.; Abu-Hassan, H.; Hassan, Z.; Al-Attar, H.A.; Monkman, A.P.; *Opt. Mater.*, **2013**, *35*, 1035. DOI: [10.1016/j.optmat.2012.12.006](https://doi.org/10.1016/j.optmat.2012.12.006)
- Riaz, M.; Song, J.; Nur, O.; Wang, Z.L.; Willander, M.; *Adv. Funct. Mater.*, **2011**, *21*, 628. DOI: [10.1002/adfm.201001203](https://doi.org/10.1002/adfm.201001203)
- Park, J.Y.; Song, D.E.; Kim, S.S.; *Nanotechnology*, **2008**, *19*, 105503. DOI: [10.1088/0957-4484/19/10/105503](https://doi.org/10.1088/0957-4484/19/10/105503)
- Joshi, P.; Chakraborti, S.; Chakrabarti, P.; Haranath, D.; Shanker, V.; Ansari, Z.A.; Singh, S.P.; Gupta, V.; *J. Nanosci. Nanotechnol.*, **2009**, *9*, 6427. DOI: [10.1166/jnn.2009.1584](https://doi.org/10.1166/jnn.2009.1584)
- Gupta, S.K.; Joshi, A.; Kaur, M.; *J. Chem. Sci.*, **2010**, *122*(1), 57.
- Zhang, N.; Yu, K.; Li, Q.; Zhu, Z.Q.; Wan, Q.; *J. Appl. Phys.*, **2008**, *103*, 104305. DOI: [10.1063/1.2924430](https://doi.org/10.1063/1.2924430)
- Gonfa, B.A.; Cunha, A.F.; Timmons, A.B.; *Phys. Status Solidi B.*, **2010**, *247*, 1633. DOI: [10.1002/pssb.200983684](https://doi.org/10.1002/pssb.200983684)
- Kim, H.; Kwon, Y.; Choe, Y.; *Nanoscale Res. Lett.*, **2013**, *8*, 240. DOI: [10.1186/1556-276X-8-240](https://doi.org/10.1186/1556-276X-8-240)
- Tian, Z.R.; Voigt, J.A.; Liu, J.; McKenzie, B.; McDermott, M.J.; Rodriguez, M.A.; Konishi, H.; Xu, H.; *Nat. Matters*, **2003**, *2*, 821. DOI: [10.1038/nmat1014](https://doi.org/10.1038/nmat1014)
- Greyson, E.C.; Babayan, Y.; Odom, T.W.; *Adv. Mater.*, **2004**, *16*, 1348. DOI: [10.1002/adma.200400765](https://doi.org/10.1002/adma.200400765)
- Sun, Y.; Fuge, G.M.; Fox, N.A.; Riley, D.J.; Ashfold, M.N.R.; *Adv. Mater.*, **2005**, *17*, 2477. DOI: [10.1002/adma.200500726](https://doi.org/10.1002/adma.200500726)
- Pan, Z.W.; Dai, Z.R.; Wang, Z.L.; *Science*, **2001**, *291*, 1947. DOI: [10.1126/science.1058120](https://doi.org/10.1126/science.1058120)
- Gao, P.X.; Wang, Z.L.; *Appl. Phys. Lett.*, **2004**, *84*, 2883. DOI: [10.1063/1.1702137](https://doi.org/10.1063/1.1702137)
- Castaneda, L.; *Acta Mater.*, **2009**, *57*, 1385. DOI: [10.1016/j.actamat.2008.11.022](https://doi.org/10.1016/j.actamat.2008.11.022)
- Yang, P.; Yan, H.; Mao, S.; Russo, R.; Johnson, J.; Saykally, R.; Morris, N.; Pham, J.; He, R.; Choi, H.-J.; *Adv. Mater.*, **2002**, *12*, 323. DOI: [10.1002/1616-3028](https://doi.org/10.1002/1616-3028)
- Ng, H.T.; Han, J.; Yamada, T.; Nguyen, P.; Chen, Y.P.; Meyyappan, M.; *Nano. Lett.*, **2004**, *4*, 1247. DOI: [10.1021/nl049461z](https://doi.org/10.1021/nl049461z)
- Lupan, O.; Pauporté, T.; Viana, B.; *Adv. Mater.*, **2010**, *22*, 3298. DOI: [10.1002/adma.201000611](https://doi.org/10.1002/adma.201000611)
- Huang, M.H.; Mao, S.; Feick, H.; Yan, H.; Wu, Y.; Kind, H.; Weber, E.; Russo, R.; Yang, P.; *Science*, **2001**, *292*, 1897.

- DOI: [10.1126/science.1060367](https://doi.org/10.1126/science.1060367)
19. Johnson, J.C.; Yan, H.; Yang, P.; Saykalley, R.J.; *J. Phys. Chem. B.*, **2003**, 107, 8816.
DOI: [10.1021/jp034482n](https://doi.org/10.1021/jp034482n)
20. Kälblein D., Ryu H., Ante F., Fenk B., Hahn K., Kern K, and Klauk H., *ACS Nano*, **2014**, 8, pp 6840–6848.
DOI: [10.1021/nn501484e](https://doi.org/10.1021/nn501484e)
21. Long Phan, T.; Yu, S.C.; Vincent, R.; Danc, N.H.; Shi, W.S.; *J. Lumin.*, **2010**, 130, 1142.
DOI: [10.1016/j.jlumin.2010.02.010](https://doi.org/10.1016/j.jlumin.2010.02.010)
22. Zhao, Q.X.; Klason, P.; Willander, M.; *Appl. Phys. A*, **2007**, 88, 27.
DOI: [10.1007/s00339-007-3958-0](https://doi.org/10.1007/s00339-007-3958-0)
23. Valerini, D.; Caricato, A.P.; Lomascolo, M.; Romano, F.; Taurino, A.; Tunno, T.; Martino, M.; *Appl Phys A*, **2008**, 93, 729.
DOI: [10.1007/s00339-008-4703-z](https://doi.org/10.1007/s00339-008-4703-z)
24. Krunks, M.; Dedova, T.; Acik, I.O.; *Thin Solid Films*; **2006**, 515, 1157.
DOI: [10.1016/j.tsf.2006.07.134](https://doi.org/10.1016/j.tsf.2006.07.134)
25. Hernández, M.A.; Álvaro, R.; Serrano, S.; Krämer, J.L.C.; *Nanoscale Res. Lett.*; **2011**, 6, 437.
DOI: [10.1186/1556-276X-6-437](https://doi.org/10.1186/1556-276X-6-437)
26. Dai, S.; Li, Y.; Du, Z.; Carter, K.R.; *J. Electrochem. Soc.*; **2013**, 160, 156.
DOI: [10.1149/2.064304jes](https://doi.org/10.1149/2.064304jes)
27. Heo, Y.W.; Varadarajan, V.; Kaufman, M.; Kim, K.; Norton, D.P.; Ren, F.; Fleming, P.H.; *Appl. Phys. Lett.*; **2001**, 81, 3046.
DOI: [10.1063/1.1512829](https://doi.org/10.1063/1.1512829)
28. Lee, J.; Easteal, A.J.; Pal, U.; Bhattacharyya, D.; *Curr. Appl. Phys.*; **2009**, 9, 792.
DOI: [10.1016/j.cap.2008.07.018](https://doi.org/10.1016/j.cap.2008.07.018)
29. Sun, J.; Gong, Y.; Liu, K.; Li, Y.; Du, G.; *Phys. status solidi A*; **2014**, 211, 625.
DOI: [10.1002/pssa.201330227](https://doi.org/10.1002/pssa.201330227)
30. Shinde, V.R.; Lokhande, C.D.; Mane, R.S.; Han, S.H.; *Appl. Surf. Sci.* **2005**, 245, 407.
DOI: [10.1016/j.apsusc.2004.10.036](https://doi.org/10.1016/j.apsusc.2004.10.036)
31. Huang, S.M.; Bian, Z.Q.; Chu, J.B.; Wang, Z.A.; Zhang, D.W.; Li, X.D.; Zhu, H.B.; Sun, Z.; *J. Phys. D: Appl. Phys.*, **2009**, 42, 055412.
DOI: [10.1088/0022-3727/42/5/055412](https://doi.org/10.1088/0022-3727/42/5/055412)
32. Park, H.K.; Oh, M.H.; Kim, S.W.; Kim, G.H.; Youn, D.H.; Lee, S.; Kim, S.H.; Kim, K.C.; Maeng, S.L.; *ETRI J.*, **2006**, 28, 787.
DOI: [10.4218/etrij.06.0206.0138](https://doi.org/10.4218/etrij.06.0206.0138)
33. Sang, N.X.; Beng, T.C.; Jie, T.E.; Fitzgerald, A.; Jin, C.S.; *Physica status solidi (a)*, **2013**, 210, 1618.
DOI: [10.1002/pssa.201228643](https://doi.org/10.1002/pssa.201228643)
34. Chu, D.; Hamada, T.; Kato, K.; Masuda, Y.; *Physica status solidi (a)*, **2009**, 206, 718.
DOI: [10.1002/pssa.200824495](https://doi.org/10.1002/pssa.200824495)
35. Jeong, J.S.; Lee, J.Y.; *Nanotechnology*; **2010**, 21, 475603.
DOI: [10.1088/0957-4484/21/47/475603](https://doi.org/10.1088/0957-4484/21/47/475603)
36. Wang, Z.L.; *Materials Today*; **2004**, 7(6), 26.
DOI: [10.1016/S1369-7021\(04\)00286-X](https://doi.org/10.1016/S1369-7021(04)00286-X)
37. Qiu, J.; Li, X.; He, W.; Park, S.J.; Kim, H.K.; Hwang, Y.H.; Lee, J.H.; Kim, Y.D.; *Nanotechnology*; **2009**, 20, 155603.
DOI: [10.1088/0957-4484/20/15/155603](https://doi.org/10.1088/0957-4484/20/15/155603)
38. Li, Q.; Kumar, V.; Li, Y.; Zhang, H.; Marks, T.J.; Chang, R.P.H.; *Chem. Mater.*; **2005**,
DOI: [10.1021/cm048144q](https://doi.org/10.1021/cm048144q)
39. Manthina V, Patel T., and Agrios A. G., *J. Am. Ceram. Soc.*; **2014**, 97, 1028.
DOI: [10.1111/jace.12947](https://doi.org/10.1111/jace.12947)
40. Liu J., She J., Deng S., Chen J., and Xu N., *J. Phys. Chem. C* **2008**, 112, 11685.
DOI: [10.1021/jp803455s](https://doi.org/10.1021/jp803455s)
41. JCPDS - International Center for Diffraction Data 1999, JCPDS File No. 36-1451.
42. Wei B., Zheng K., Yuan J, Zhang Y., Zhang Z, and Han X.; *Nano Letters*, **2012**, 12, 4595.
DOI: [10.1021/nl301897q](https://doi.org/10.1021/nl301897q)
43. Nikoobakht B., Eustis S., and Herzing A.; *J. Phys. Chem. C*, **2009**, 113 7031.
DOI: [10.1021/jp810831z](https://doi.org/10.1021/jp810831z)
44. Zhang Z. Y, *Physics Letters A*, **2014**, 378, 1174.
DOI: [10.1016/j.physleta.2014.02.029](https://doi.org/10.1016/j.physleta.2014.02.029)
45. Hsua, H.C.; Tseng, Y.K.; Cheng, H.M.; Kuo, J.H.; Hsieh, W.F.; *J. Cryst. Growth*; **2004**, 261, 520.
DOI: [10.1016/j.jcrysgro.2003.09.040](https://doi.org/10.1016/j.jcrysgro.2003.09.040)
46. Kim, M.S.; Yim, K.G.; Leem, J.Y.; *J. Korean. Phys. Soc.*; **2011**, 59 (3), 2354.
DOI: [10.3938/jkps.59.2354](https://doi.org/10.3938/jkps.59.2354)



A Monthly Journal

Publish your article in this journal

Advanced Materials Letters is an official international journal of International Association of Advanced Materials (IAAM, www.iaamonline.org) published monthly by VBRI Press AB from Sweden. The journal is intended to provide high-quality peer-review articles in the fascinating field of materials science and technology particularly in the area of structure, synthesis and processing, characterisation, advanced-state properties and applications of materials. All published articles are indexed in various databases and are available download for free. The manuscript management system is completely electronic and has fast and fair peer-review process. The journal includes review article, research article, notes, letter to editor and short communications.

www.vbripress.com/aml

Copyright © 2016 VBRI Press AB, Sweden